

# Live Cell Analysis of Scratch Wound Migration and Invasion Assays using the Agilent xCELLigence RTCA eSight

## Authors

Tian Wang, Xiaoyu Zhang,  
Ryan Raver, Peifang Ye, and  
Yunfei Pu  
Agilent Technologies, Inc.

## Abstract

Migration and invasion are key properties of live cells and critical for normal development, immune response, and pathological processes such as cancer metastasis. Methods to examine cell migration and invasion are useful and important for a wide range of biomedical research fields, such as cell biology and developmental biology, immunology, and cancer biology. The scratch assay (also called wound healing assay) is a straightforward and economical method to study cell motility in vitro. The principle behind this method is based on the creation of an artificial "scratch", disrupting the cell confluent monolayer. The outer layer or peripheral cells then attempt to "heal" the artificially created wound or gap in the center. Traditionally, many manual scratching tools (for example, pipette tips) have made it difficult to standardize a wound's width, direction, and position. In this study, an optimized Agilent AccuWound 96 scratch tool was used to create consistent and reproducible scratches in monolayer cells to overcome the imitations of conventional methods. Real-time, automatic live cell imaging on the Agilent xCELLigence RTCA eSight quantifies the speed of wound closure. This application note demonstrates the simplicity, precision, and continuity of signal recording of the xCELLigence RTCA eSight, enabling visualization and simple quantification of cell migration and invasion, and assessment of morphological changes in real time.

## Introduction

Motility is an essential feature of live cells. Cell migration involves a complex, multistep process, and is initiated by stimuli that activate a set of signaling pathways, leading to cell polarization and rapid recombination of actin filaments and microtubules.<sup>1</sup> The cell membrane protrudes at the boundary of the precursor cell, causing the cell to move forward, followed by dynamic substrate adhesion by way of integrin adhesion to the substrate. The edge of the cell membrane then contracts to complete one cycle, and repeats in rapid succession, causing the cell to migrate.<sup>2,3</sup> Furthermore, cell migration is involved in the conception of life, embryonic development, immune response, and many pathological processes such as cancer metastasis and inflammation.<sup>4</sup> Therefore, methods to study cell migratory behavior are useful research tools in biomedical sciences, biology, bioengineering, and related fields.

Cell invasion is the ability of a cell to migrate by degrading the extracellular matrix. Cell invasion is the response of normal cells and cancer cells to chemical and mechanical stimuli, often occurring in wound repair, angiogenesis, inflammatory reaction, abnormal tissue infiltration, tumor cell metastasis, and other processes. Cancer cell migration and invasion play an integral part in metastatic disease and are a leading cause of death in cancer patients.<sup>5</sup>

The in vitro scratch wound healing assay is an easy, low-cost, and well-developed method to study cell migration and invasion.<sup>6</sup> In this particular assay, cells are grown to confluence and then "scratched" with a sterile instrument. The acellular area is formed by a scratch, which becomes the wound area. The resulting polarity from the cells in the leading edge induces migration or invasion across a Matrigel layer to "heal" the modeled wound.<sup>6,7</sup> The degree and rate of wound healing provide information about motility characteristics, cell health, and the ability to interact with other cells. Manual methods, such as the use of pipette tips, lack reproducibility and introduce numerous variables.<sup>8</sup> Therefore, standardizing a wound's width, direction, and position is crucial to efficiently monitor and accurately measure cell migration.

This application note demonstrates the use of the AccuWound 96 scratch tool to create consistent and reproducible scratches, spanning monolayers formed by multiple cell types, at the base of each well in a 96-well plate. Wound healing rates are automatically measured and captured in real time by the xCELLigence RTCA eSight using live cell imaging and the **Wound Healing License and software module**.

## Assay principle

The Agilent xCELLigence RTCA eSight is currently the only instrument that combines live cell imaging with highly sensitive cell impedance to monitor cell health and behavior in real time. The core of the eSight system is a dedicated microelectronic detection microplate (E-Plate) with gold biosensors arrayed on the glass bottom surface, which can continuously and noninvasively monitor cell impedance. The eSight has five cradles, of which cradles 1, 2, and 3 collect both impedance and imaging data simultaneously and are only suitable for specialized gold biosensor cell plates (E-Plates); cradles 4 and 5 are suitable for regular cell culture plates and only collect imaging data. This application note demonstrates the use of cradles 4 and 5 only, and an image-specific scratch wound application.

Specifically, when the cells reach confluence in each well, the plate is placed in the tool and a knob is turned to control a spring-loaded polytetrafluoroethylene (PTFE) pin across the bottom of each well. Ninety-six uniform and highly reproducible scratches are generated. The latest Agilent AccuWound 96 scratch tool Model 2000 (part number 380601420) is optimized for compatibility with regular polystyrene or more sensitive 96-well plates, resulting in cleaner wound areas and avoidance of surface material scratches.

Using the eSight's **Wound Healing software module**, the closure of the wound through cell migration was recorded in real time and analyzed. The simple workflow is shown in Figure 1.

Both migration and invasion assays are conducted on a 96-well cell culture microplate in cradles 4 and 5 (Figure 1). One distinction lies with the invasion assay, where a layer of extracellular matrix (ECM) is put on the cell layer (and cell migration is in the absence of Matrigel). Cell migration or cell invasion is then imaged. The eSight software processes the images under a refined processing definition. Wound areas are then recognized, and multiple metrics are provided to quantify cell migration and invasion over time.

The xCELLigence RTCA eSight allows detection in both brightfield and three fluorescent channels (red, green, and blue) and provides metrics for fluorescence channels (see details in the eSight software user manual).

## Migration/invasion assay quick guide

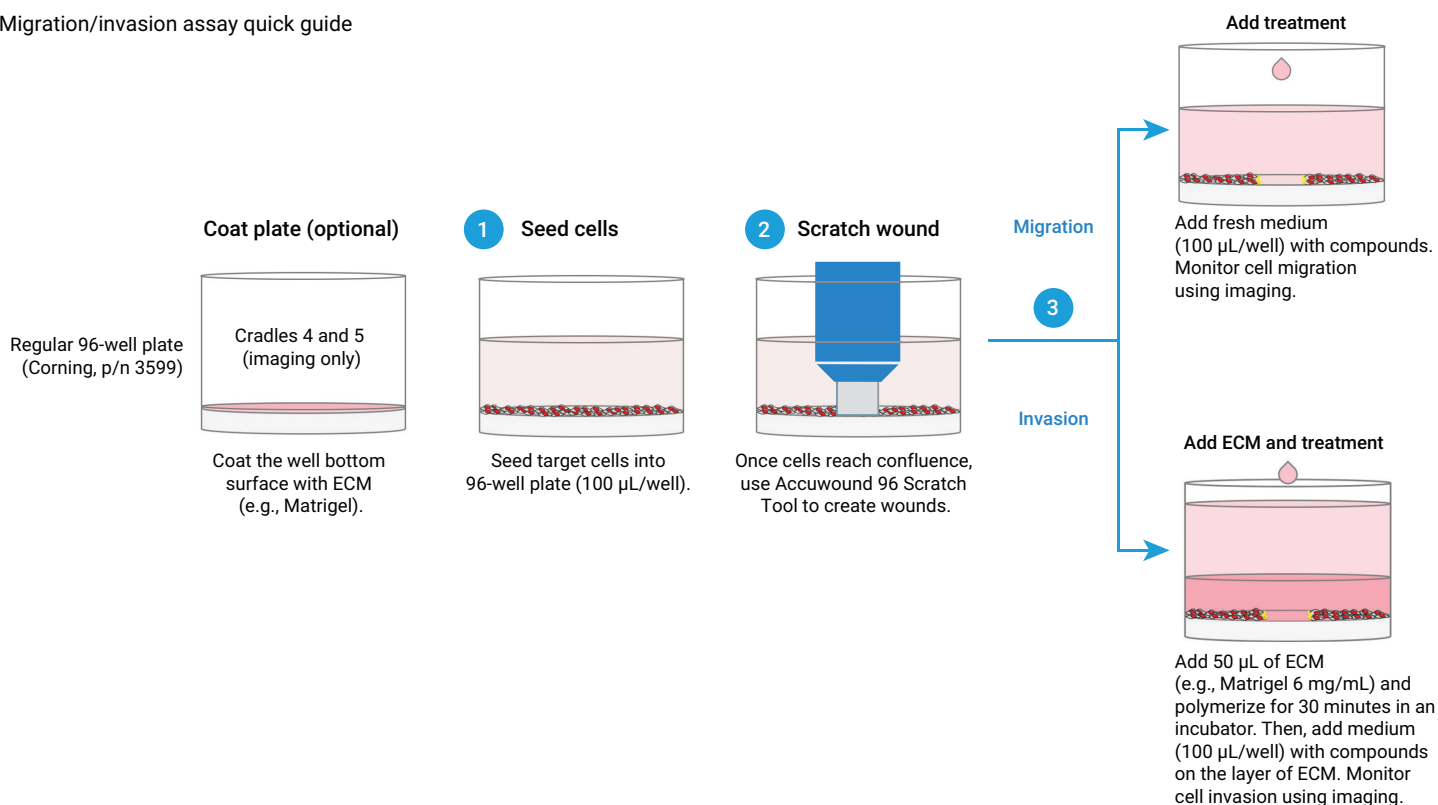


**Figure 1.** Workflow for migration and invasion assays using the Agilent xCELLigence RTCA eSight system.

## Materials and methods

### Cells, medium, and growth conditions

Cell culture maintenance and assays were performed in an incubator (37 °C/5% CO<sub>2</sub>). Cell lines and their growth media are shown in Table 1.

**Table 1.** Cell lines and growth media.

Cell Line	Part Number	Base Medium
HT-1080	ATCC, part number CCL-121	EMEM (ATCC, part number 30-2003)
A549	ATCC, part number CCL-185	F-12K media (Gibco, part number 21127-022)
SKOV3	ATCC, part number HTB-77	McCoy's 5A (Gibco, part number 16600-082)
Hs27	ATCC, part number CRL-1634	DMEM (ATCC, part number 30-2002)
MCF7	ATCC, part number HTB-22	EMEM (ATCC, part number 30-2003)
HeLa	ATCC, part number CCL-2	EMEM (ATCC, part number 30-2003)
MDCK	ATCC, part number CCL-34	RPMI 1640 (Gibco, part number 11875-093)

All the listed media in Table 1 were supplemented with 10% FBS (Gibco, part number 16050-122) and 1% Pen/Strep (HyClone, part number SV30010) for cell growth.

### Cell preparation and cell seeding

Seven cell lines are used in this study. The preparation of SKOV3 NucRed cells is described here as an example. SKOV3 NucRed (SKOV3-Red) is a stable nuclear red-labeled cell line, which was generated by transducing parental cells with Agilent eLenti Red reagent (part number 8711011) and subsequent short puromycin selection. The cells were seeded at 40,000 cells/well by adding 100 µL of cell suspension to each well of a 96-well plate (Corning, part number 3599). The cells were allowed to settle in the plate for 30 minutes at room temperature for even distribution. Image acquisition was initiated to monitor cell adhesion and proliferation.

## Cell migration and invasion assays

Before using the AccuWound 96 scratch tool, the scratch pins were sterilized. The well bottom surface of a regular 96-well plate was coated with a thin layer of extracellular matrix (ECM, 100 µg/mL Matrigel, Corning).

**Note:** The coating step is optional, helping the cells adhere quickly to the well bottom so the scratching step can be performed on the same day as cell seeding. Without coating, the scratching step needs to be performed the day after cell seeding when the cells are strongly attached to the bottom surface.

Once cells were attached and reached confluence (observed confluence from the images), data acquisition was paused, and the plate was transferred into a sterile tissue culture hood that contained the sterilized AccuWound 96 scratch tool. The knob was turned to slide the spring-loaded PTFE pin across the bottom of each plate well to generate scratch wounds. Debris-containing media from the scratched wells were removed with two gentle washes and 200 µL of prewarmed fresh media.

**Migration assay:** Following washing, 100 µL of media containing a series of concentrations of Cytochalasin D (Cyto D) (3 µM, 1.5 µM, 0.75 µM, 375 nM, 187.5 nM, 93.75 nM, 46.88 nM, 23.44 nM, and 11.72 nM) was added into the wells. The plate was placed back in cradle 4 or 5, and images were captured once per hour using the 10x objective. The instrument automatically adjusted the brightfield settings, while exposures in red were manually set to 300 ms.

**Invasion assay:** After washing, the plate was placed on ice and allowed to equilibrate for 5 minutes. Then, 50 µL/well of 6 mg/mL Matrigel matrix (Corning, part number 354248) was added to each well of the 96-well microplate and gel at 37 °C for 1 hour. Note that Cyto D was diluted to its final concentration (mentioned above in the migration assay) in the gel layer, and all microplates or media containing Matrigel should be prechilled/ice-cold during operation. After ECM was overlaid with 100 µL of complete medium containing the Cyto D, the plate was placed back on cradle 4 or 5 of the eSight system and was imaged once per hour using the 10x objective. While brightfield settings were automatically adjusted by the instrument, exposures in red were manually set to 300 ms.

**Primary metrics:** The eSight software processes wound healing images under an optimized processing definition. Wound areas are recognized during imaging processing, and multiple metrics are provided to quantify cell migration and/or invasion over time. Wound cell area, wound confluence, and wound width are described here (please see the eSight software manual or the software interface for the complete metrics list).

Wound width is calculated using the following equation:

$$\text{Wound width } (\mu\text{m}) = \frac{\text{image area} - \text{recognized cell area}}{\text{wound length}}$$

Wound confluence (%), also known as wound healing %, is calculated based on the percentage of wound cell area (mm<sup>2</sup>) to the initial wound area. Wound width (µM) is the average distance between the boundaries of the wound area (Figure 2A).

## Results and discussion

### Quantification of wound healing using various primary imaging metrics

After SKOV3 cells were seeded, a wound was created after six hours. Initial wound area (t = 0 hours) was first calculated, which is masked in yellow (Figure 2A). During cell migration, the initial wound area covered with migrated cells is known as the wound cell area (Figure 2A). As the initial wound area or gap closed, wound width and wound confluency were calculated in real time (Figure 2A; t = 15 and 30 hours).

In addition to the primary metrics, the wound healing rate can also be directly calculated by the eSight software through the slope of these metric curves. Figure 2B shows the wound healing rate of 94,808 µm<sup>2</sup>/hour, which is calculated based on the kinetics of the wound cell area curve between 0 and 24 hours.

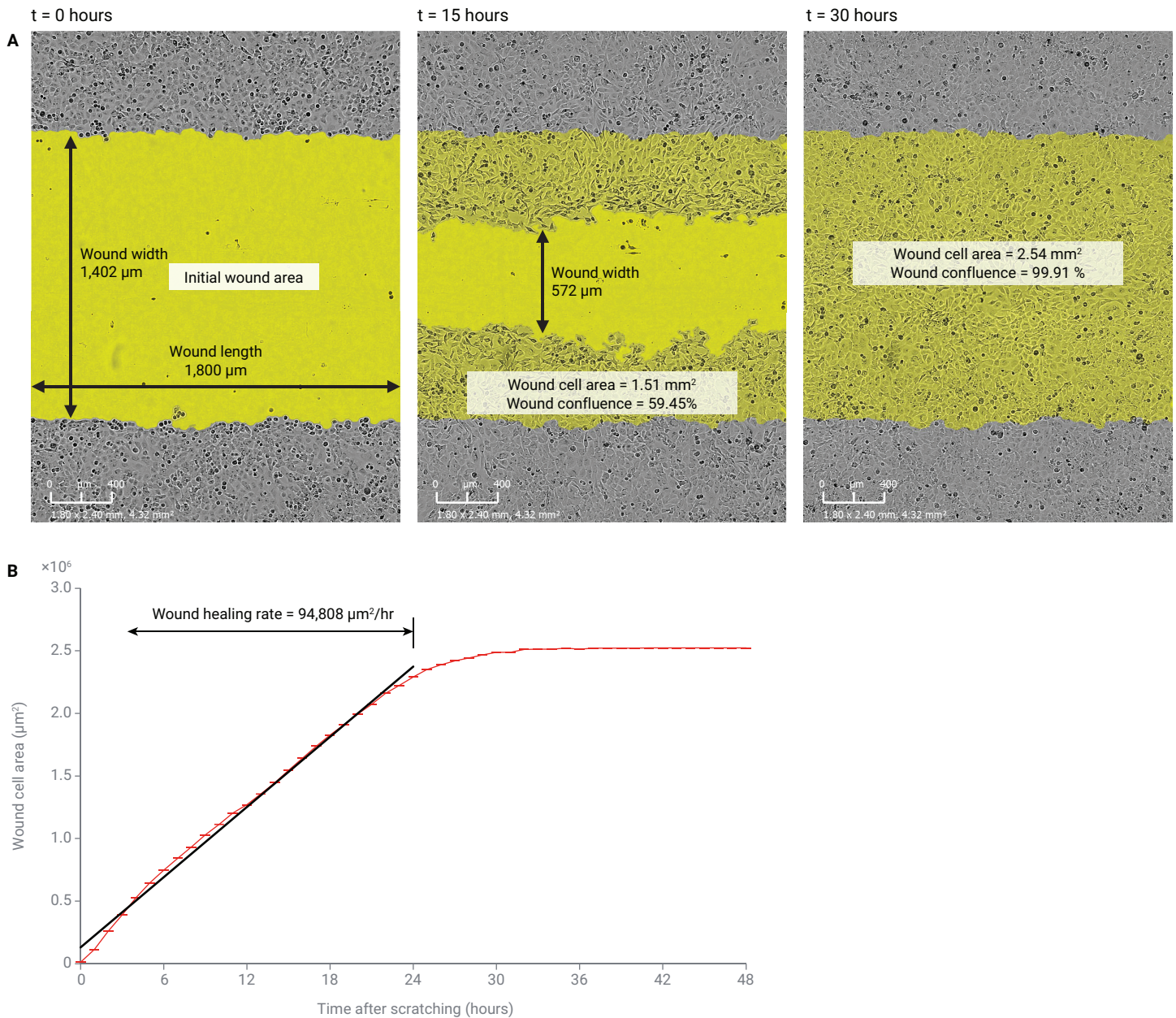


**Figure 2.** Quantifying cell migration or invasion: SKOV3 cells were seeded at a density of 40,000 cells/well, and the wound was generated six hours after cell seeding. (A) The initial wound area (t = 0 hours) and wound cell areas were recorded by the eSight system and quantified by the eSight software at t = 15 and 30 hours. The wound cell area is the region now covered by cells that have invaded/migrated into the initial wound area. The pure yellow region indicates the region of the wound that is still cell-free. The wound confluence is the percentage of wound cell area to the initial wound area. Wound width is the average distance between the boundaries of the wound (the pure yellow area). (B) Representative data showing the wound cell area versus time. The slope of the curve, which indicates the wound healing rate, was calculated in the eSight software based on the time range of 0 to 24 hours.

**Scratch wound creation and different migration capacities of various cell types quantified by brightfield-based imaging**

The Wound Healing Module of xCELLigence RTCA eSight is suitable for most adherent cells without labeling. Not surprisingly, the wound boundary characteristics and wound healing rates of different cell lines vary. Figure 3 shows initial wounds and wound healing at 24 hours after scratching on different types of tumor cells, human fibrosarcoma cell HT-1080, Madin-Darby canine kidney cell MDCK, ovarian cancer cell SKOV3, skin cancer cell Hs27, cervical cancer cell HeLa, breast cancer cell MCF7, and non-small cell lung cancer cell A549. The initial wound boundaries are indicated in yellow and have a nice linear pattern for all cell types, except MDCK cells. MDCK cells are widely used as models for studying epithelia as they have clear apical-basolateral polarity, well-defined cell junctions, and a rapid growth rate.<sup>8</sup> The situation of MDCK here clearly reflects its characteristics. HT-1080 and MDCK cells healed completely at 24 hours

after the scratch, whereas HeLa, MCF7, and A549 cells show weak mobility. SKOV3 and Hs27 cells display a mid-degree of mobility. Although the cell line generates a characterized wound boundary, the eSight software still accurately demarcates each cell's wound boundaries (cyan segmentation masks in Figure 3 at 24 hours).

**Evaluating the inhibitory effect of Cytochalasin D on SKOV3-Red cell migration by both brightfield and red fluorescent imaging**

As shown in Figure 4, SKOV3-Red cells were treated with serial concentrations of Cyto D, and imaging was recorded over 48 hours at 1-hour intervals. As expected, this migration inhibition response is dose-dependent, with the highest Cyto D concentration causing the most pronounced inhibition. After 24 hours, the wound confluence in the control group (DMSO group) reached 91.3%, while that in the 187.5 nM Cyto D group was only 15.8%.

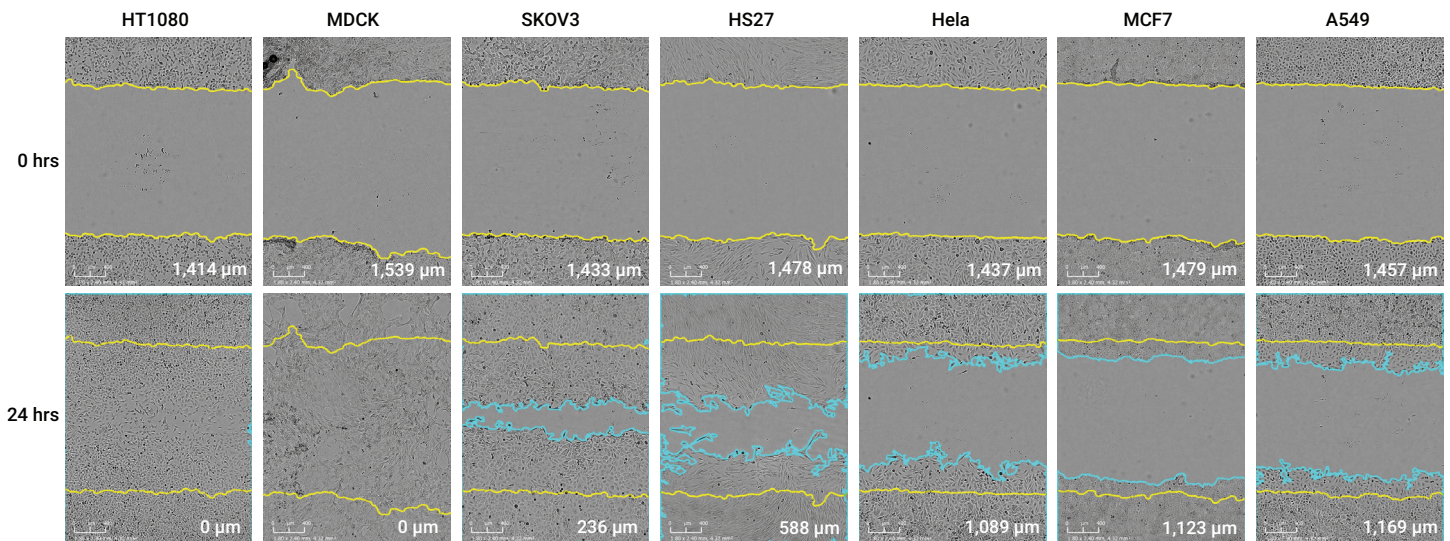


**Figure 3.** Label-free monitoring of wound closure over time for various cell lines. The initial wound boundary is indicated in yellow; the wound boundary at 24 hours post-scratch generation is indicated in cyan (if present). The wound width of each image is recorded at the right corner.

+ Cytochalasin D (nM)

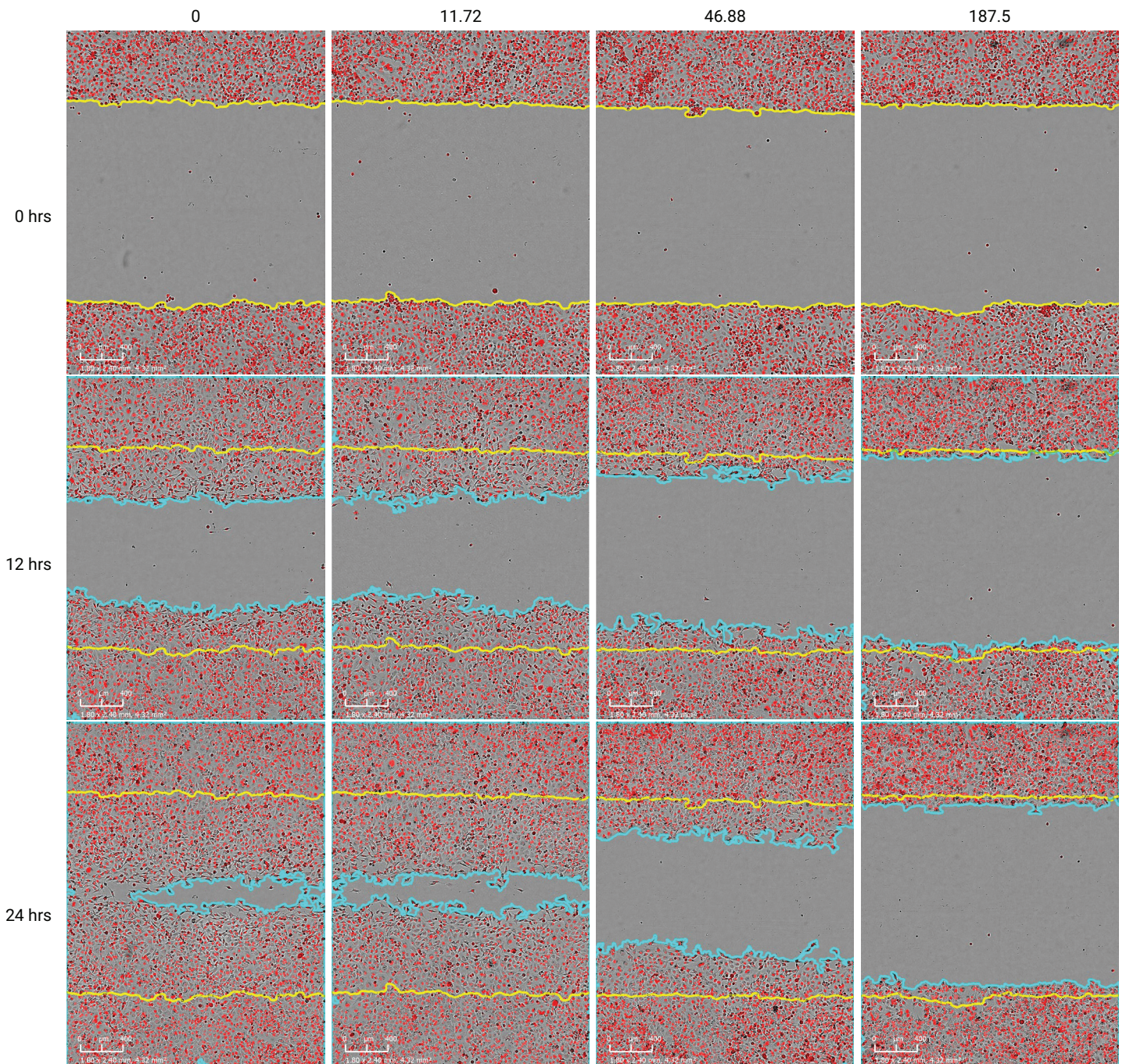


**Figure 4.** Cytochalasin D inhibited SKOV3 cell migration in a concentration-dependent manner. Scratched SKOV3 Red cells were treated with different concentrations of Cytochalasin D. Agilent eSight collected images once per hour, and representative images were taken at 0, 12, and 24 hours post-scratch.

The inhibition of cell migration by Cyto D was quantified using the brightfield wound confluence and red wound count (for example, the red nuclei count of the initial wound area). Plotting either the wound confluence (Figure 5A) or the red wound count (Figure 5B) of the SKOV3 cells both clearly demonstrate a dose-dependent migration inhibition by the actin polymerization inhibitor Cyto D.

Figure 5C shows the dose-response curve (DRC) for the previously mentioned parameters. The  $IC_{50}$  values of Cyto D on SKOV3 for wound confluence and red wound count are similar, 50.77 and 41.77 nM, respectively, as the quantitative parameters are both equally reliable. The use of multiple imaging channel detection methods provides additional information richness and confidence.

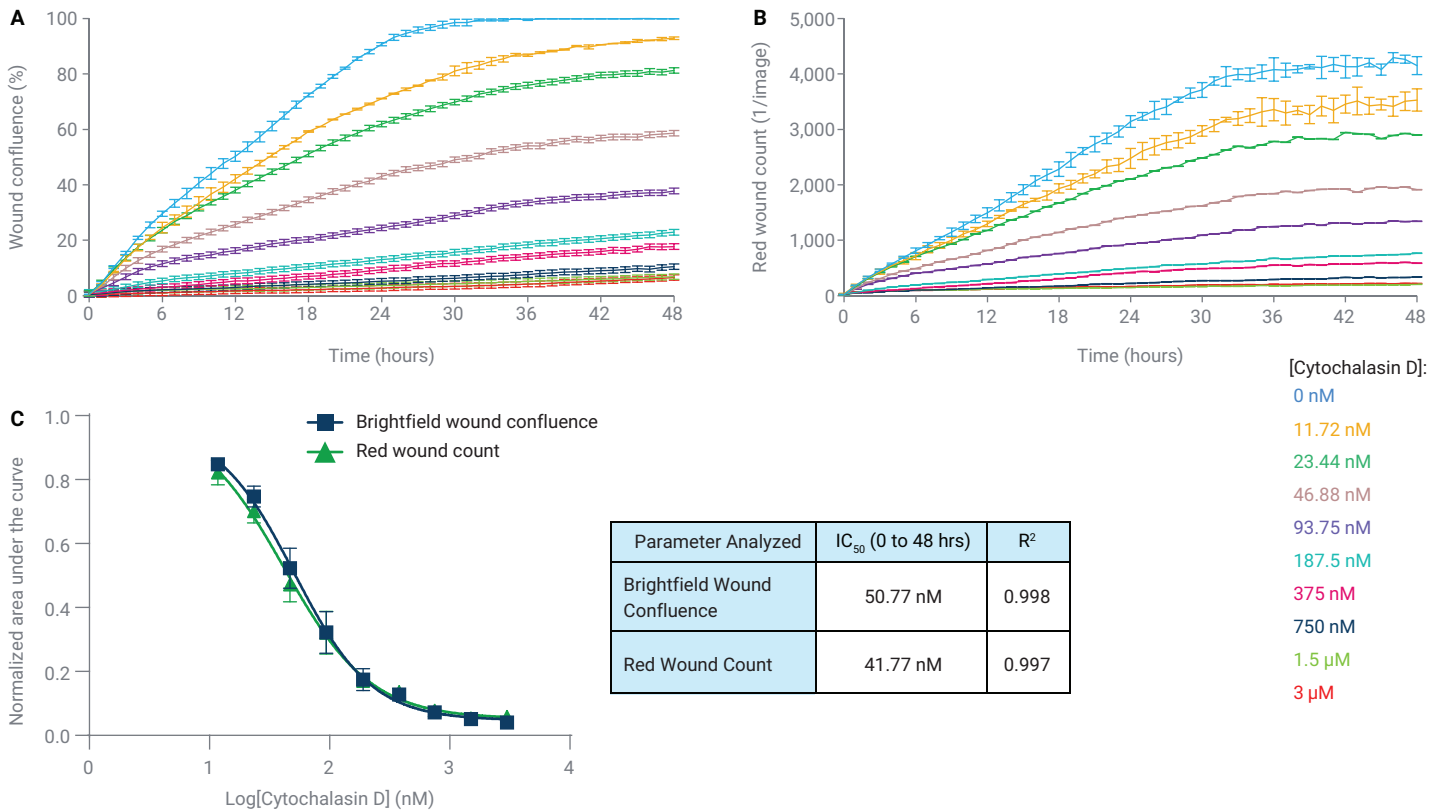


**Figure 5.** Quantitative analysis of the inhibitory effect of Cytochalasin D on SKOV3 cell migration. (A) Wound confluence as a function of time. (B) The number of (red) nuclei in the initial wound area as a function of time. (C) Dose-response curves (DRC), and  $IC_{50}$  values calculated from the DRCs. Area under the curve (AUC) values were normalized using the following equation: Normalized AUC = AUC/AUC vehicle control.



### Differences in HT-1080 morphology and rate of wound closure between migration and invasion assays

HT-1080 cells were also treated with different concentrations of Cyto D from 3  $\mu\text{M}$  to 11.72 nM (two-fold concentration gradient), and cell migration and invasion assays were performed. As shown in Figure 6, there are vast differences in wound closure rates and cell morphology between the

migrating and invading HT-1080 cells. The HT-1080 cells migrated to close the wound region at a significantly higher rate, with complete wound closure detected around 24 hours post-scratching in the absence of Cyto D, while HT-1080 cell invasion within 6 mg/mL Matrigel only reached 59.6% wound closure.

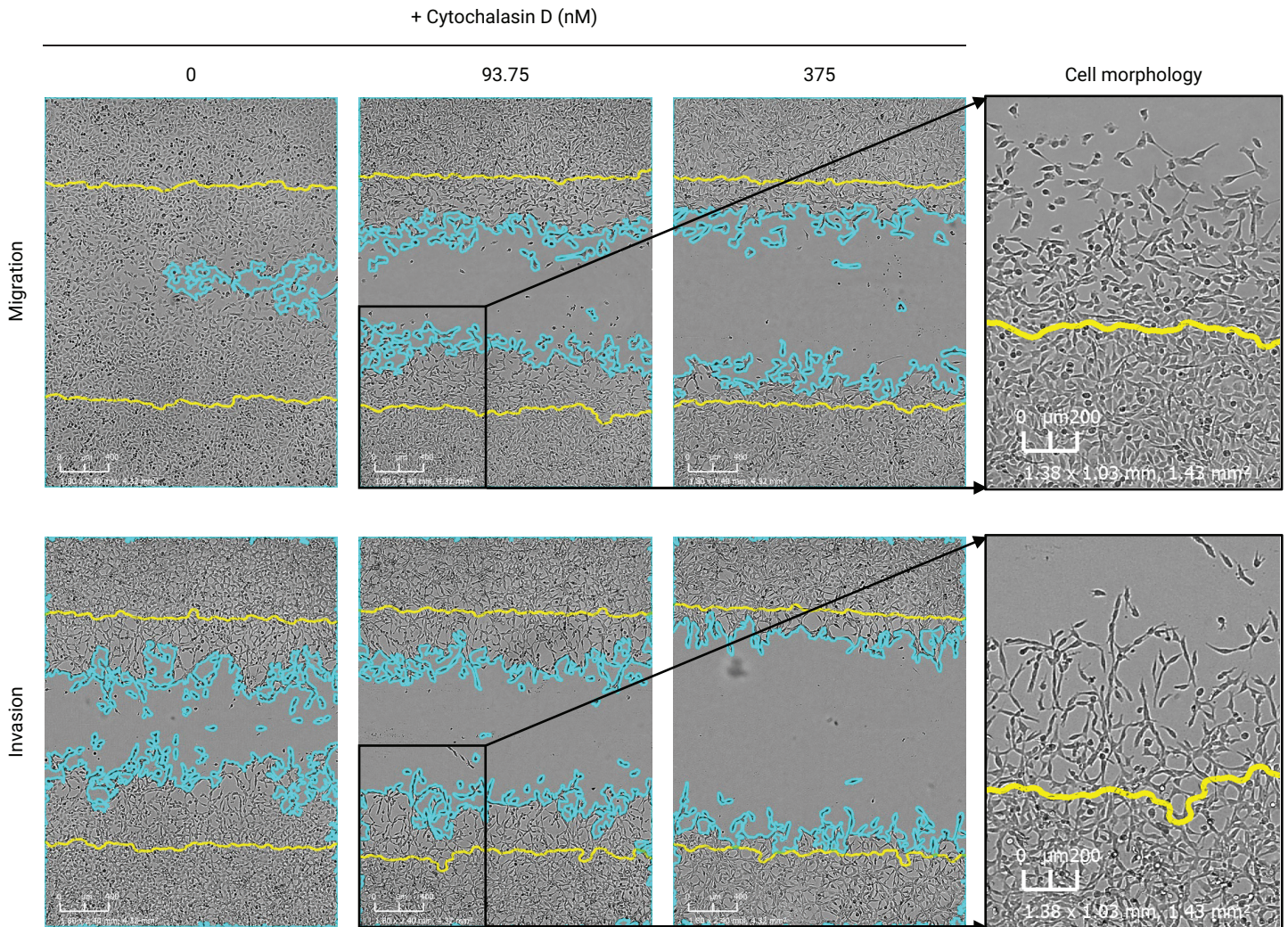


**Figure 6.** Representative images show the dose-dependent inhibitory effect of Cytochalasin D on HT-1080 cell migration and invasion. Images were collected in an Agilent eSight system once per hour. Representative images taken 24 hours post-wound generation are shown. The cell invasion rate is lower than the migration rate. In addition, typical cell morphology during cell migration or invasion is also magnified and shown on the far right.

Significant differences in cell morphology were also shown in Figure 6. The migrating cells still maintained the original fiber shape of the cells, with round pseudopodia, and the cell group moved forward uniformly. The invading HT-1080 cells, however, had a mesenchymal phenotype with "spike-like" invadopodia, and the cells advanced in an "invading" manner.<sup>10</sup> However, both exhibited the Cyto D dose-dependent inhibition effect.

To compare the wound healing rate between migration and invasion intuitively, wound confluence based on representative images in the migration and invasion assays was plotted as a function of time (Figure 7). Plotting the area under these curves in each assay versus the Cyto D concentration produced the dose-response curves in Figure 7B, and the  $IC_{50}$  of Cyto D on HT-1080 cell migration and invasion for wound confluence (256 nM versus 196 nM, respectively). Not surprisingly, the wounds in the migration assay close faster than in the invasion assay (Figures 7A and 7C). The close  $IC_{50}$ s show that the inhibitory efficacy of Cyto D on migration and invasion is similar (Figure 7B).

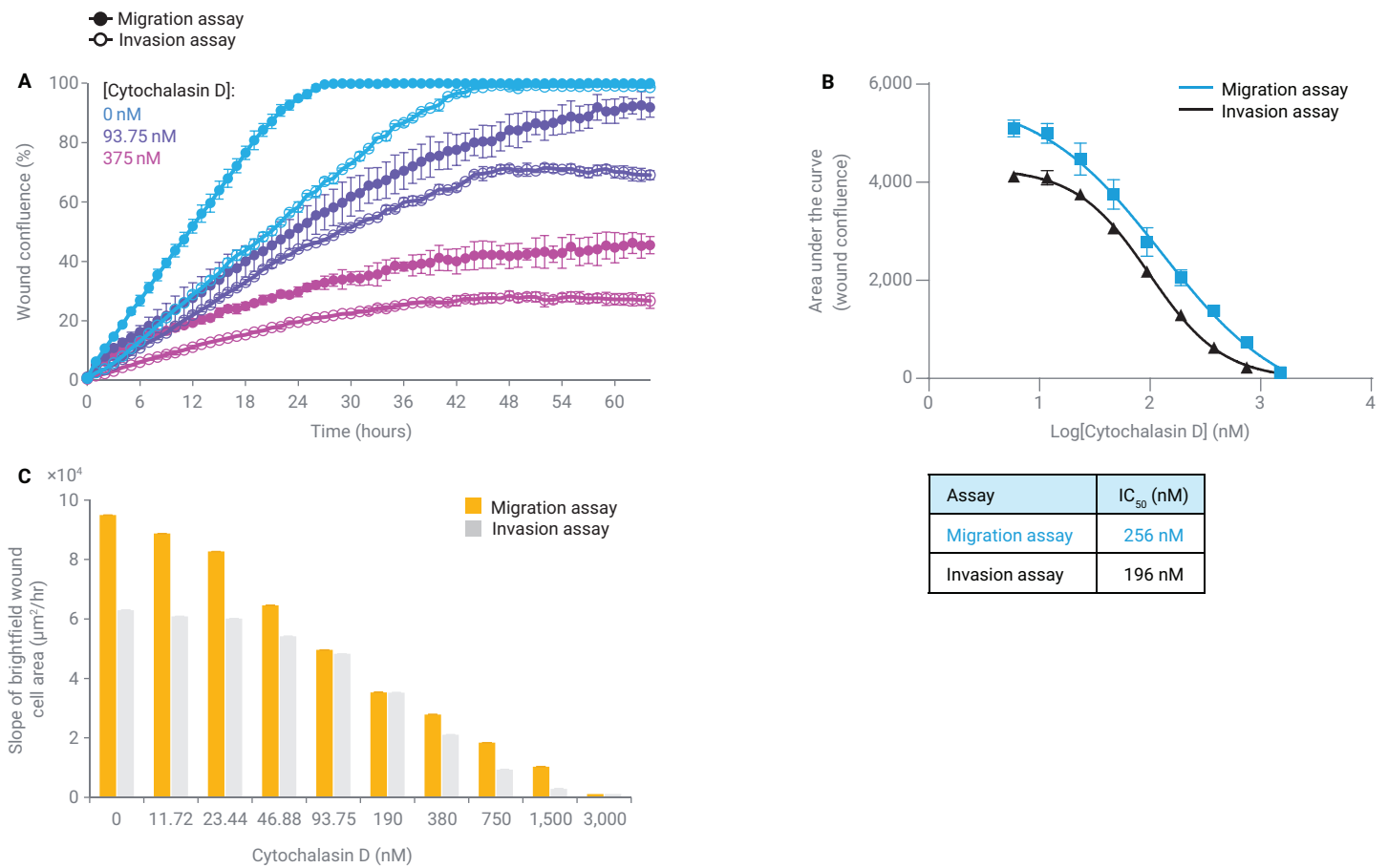


**Figure 7.** Quantitative analysis of the inhibitory effect of Cytochalasin D on the migration and invasion of HT-1080 cells. (A) Wound confluence as a function of time for the migration and invasion assays. (B) Dose response curves for migration and invasion assays as a function of Cytochalasin D concentration. (C) The slope of wound cell area (0 to 24 hours post scratch) for migration and invasion assays as a function of Cytochalasin D concentration.

## Conclusion

Monitoring cell mobility plays a key role in understanding the multistep process of metastasis, adhesion, and invasion in cancer treatment. The Wound Healing Module of the Agilent xCELLigence RTCA eSight system provides a simple, around-the-clock method for monitoring of cell migration and invasion in real time using imaging. Parameters such as wound confluence (as wound healing percentage), wound width, and wound cell area on the eSight provide deeper biological insights and significantly less hands-on time compared to manual quantifying procedures using ImageJ software. Of note, image-based quantitative analysis requires that users manually input and optimize various parameters such as the background and cell size range, which is critical for good recognition and subsequent analysis.

Although imaging was the focus of this application note, Cell Index (not shown) is yet another readout that can be measured and quantified for cell migration and invasion, particularly for xCELLigence RTCA instrumentation (eSight cradles 1 to 3 only, MP, SP, and DP). Cell Index has certain advantages with rapid kinetics (a few seconds per 96-well plate), high sensitivity, and objective data (without the need for processing or input from the user). Please see the [AccuWound 96 User Manual](#) for more information.

Lastly, the xCELLigence RTCA eSight can be widely used to detect the migration and invasion ability of most adherent cells. The migration-related phenotypes determined by the eSight provide useful information about the metastatic potential of certain types of cancer studied *in vivo* for the prognosis of the disease or to evaluate the function of tested substances (such as drugs) in changing cell migration/invasion. Such real-time, live cell analysis-based assays will continue to help fuel preclinical based studies and evaluate efficacy.

## References

1. Welf, E. S.; Haugh, J. M. Signaling Pathways that Control Cell Migration: Models and Analysis. *Wiley Interdiscip. Rev. Syst. Biol. Med.* **2011**, *3*(2), 231–240. doi:10.1002/wsbm.110.
2. SenGupta, S.; *et al.* The Principles of Directed Cell Migration. *Nature Reviews. Molecular cell biology* **2021**, *22*(8), 529–547. doi:10.1038/s41580-021-00366-6.
3. Abercrombie, M. The Croonian Lecture, 1978: The Crawling Movement of Metazoan Cells. *Proceedings of the Royal Society of London, Series B. Biological Sciences* **1980**, *207*(1167), 129–47. JSTOR, <http://www.jstor.org/stable/35404>.
4. Vicente-Manzanares, M.; Horwitz, A. R. Cell Migration: an Overview. *Methods in Molecular Biology* (Clifton, N.J.) **2011**, *769*, 1–24. doi:10.1007/978-1-61779-207-6\_1.
5. Kramer, N.; *et al.* In Vitro Cell Migration and Invasion Assays. *Mutation Research* **2013**, *752*(1), 10–24. doi:10.1016/j.mrrev.2012.08.001.
6. Liang, C.-C.; *et al.* In Vitro Scratch Assay: a Convenient and Inexpensive Method for Analysis of Cell Migration In Vitro. *Nature Protocols* **2007**, *2*(2), 329–33. doi:10.1038/nprot.2007.30
7. Rodriguez, L. G.; *et al.* Wound-Healing Assay. *Methods in Molecular Biology* (Clifton, N.J.) **2005**, *294*, 23–9. doi:10.1385/1-59259-860-9:023.
8. Cormier, N.; *et al.* Optimization of the Wound Scratch Assay to Detect Changes in Murine Mesenchymal Stromal Cell Migration After Damage by Soluble Cigarette Smoke Extract. *Journal of Visualized Experiments: JoVE* Dec. 3 **2015**, *106*, e53414. doi:10.3791/53414.
9. The European Collection of Authenticated Cell Cultures (ECACC). Cell Line Profile of MDCK[EB/OL]. (2021-12-14)[2023-6-7]. <https://www.culturecollections.org.uk/media/137096/mdck-cell-line-profile.pdf>.
10. Kim, S.-K.; *et al.* Phenotypic Heterogeneity and Plasticity of Cancer Cell Migration in a Pancreatic Tumor Three-Dimensional Culture Model. *Cancers* May 21 **2020**, *12*(5), 1305. doi:10.3390/cancers12051305

[www.agilent.com/chem/esight](http://www.agilent.com/chem/esight)

For Research Use Only. Not for use in diagnostic procedures.

RA45229.3533680556

This information is subject to change without notice.

© Agilent Technologies, Inc. 2023  
Printed in the USA, December 8, 2023  
5994-6887EN